The empirical corner stiffness for right-angle frames of rectangular and H-type cross-sections

Young-Doo Kwon[*1], Soon-Bum Kwon[1a], Hyuck-Moon Gil[2b] and Hui-Jeong Cho[3c]

[1]*School of Mechanical Engineering & IEDT, Kyungpook National University, Daegu, Korea*
[2]*Department of Offshore Structure Design & Engineering, Hyundai Heavy Industry, Ulsan, Korea*
[3]*Graduate School, Kyungpook National University, Daegu, Korea*

Abstract.   Until now, the finite corner stiffness of the right-angle frames used as horizontal girders in a bonnet, have not been considered during the design process to result in not a precise result. This paper presents a design equation set for right-angle frames used as horizontal girders in a bonnet assuming rigid corner stiffness. By comparing the center stresses of the right-angle frame according to the design equation set with the results of the finite element method, the master curves for the empirical corner stiffness can be determined as a function of slenderness ratio. A second design equation set for a right-angle frame assuming finite corner stiffness was derived and compared with the first equation set. The master curves for the corner stiffness and the second design equation set can be used to determine the design moments at the centers of the girder so that the bending stresses can be analyzed more precisely.

Keywords: frame; bonnet; slide gate; wide flange beam; slenderness ratio; corner stiffness; master curves

1. Introduction

The continued growth of industry and improvement in living standards have placed new demands on water supplies. In particular, large barrages for dam construction, which can be several kilometers in length, are being operated for balanced national development and the efficient use of water resources in many countries (Shariatmadar 2011). A key component of a dam is the gate used to control the flow rates and adjust the water level. Many types of gates with their own characteristics have been developed. The slide gate is typically small in size. Although it has a high operating resistance, it has a simple structure and relatively low installation cost (Lewin 2001, Hydraulic and Penstock Association 1986).

High-pressure gates first appeared with the successful application of the jet flow gate at Shasta Dam in the 1940s, and many similar types have been attempted by the US Army Corps of Engineers. Similar structures include the ring follower gate, jet flow gate, and roller gate (Kwon *et*

---

*Corresponding author, Professor, E-mail: ydkwon@knu.ac.kr
[a]Professor, E-mail: sbkwon@knu.ac.kr
[b]Researcher, E-mail: hmoon77@hanmail.net
[c]Graduate school, E-mail: queen8511@naver.com

al. 2000, Kwon *et al*. 2004). These gates all have the structure of a bonnet wrapped around the gate. The bonnet of the slide gates is loaded by the internal water pressure. Although an accurate evaluation of the corner moment is very important, current design concepts for the bonnet of a slide gate are inadequate as they are based on an infinite corner stiffness for frames (Timoshenko and Goodier 1970, Reismann and Pawlik 1980, Ugural and Fenster 2003).

This paper proposes two master curves for the empirical determination of the corner stiffness in combination with a theory based on the assumption of finite stiffness (Kwon). The empirical corner stiffness was reverse-engineered from the deviation of stresses obtained assuming infinite corner stiffness and by the finite element method (FEM). The accuracy of the new procedure for stress analysis of a right-angle frame was tested and confirmed through a comparison of the resulting stresses with the FEM results. The proposed master curves for the empirical corner stiffness were successfully applied to the analysis and design of a right-angle frame in conjunction with the theory of the finite referred corner stiffness.

2. Structure of bonnet and design equations for right-angle frames

A bonnet is used in a high-pressure slide gate installed deep underwater to resist high water pressures and is composed of skins and horizontal girders in the shape of a right-angle frame. In the design of a right-angle frame, the stiffness of the corner was assumed to be rigid; the corresponding corner moment was confirmed based on this assumption. Using this corner moment, the center moments were calculated to evaluate the maximum bending stresses.

However, these stresses sometimes deviated considerably from the finite element analysis (FEA) results. After an extensive trial-and-error process, the deviation seemed to be rooted in the inaccurate assumption of infinite corner stiffness. To resolve this problem, the finite corner stiffness was evaluated empirically based on the deviation of stresses. For a given cross-section of a right-angle frame, a master curve can be obtained as a function of the slenderness ratio regardless of the dimensions. More accurate center moments of the right-angle frame and the corresponding accurate stresses can be obtained by using this corner stiffness and referring to the design equation assuming finite corner stiffness.

2.1 Structure of bonnet

Fig. 1 shows the entire bonnet structure of a high-pressure slide gate. The role of the gate is to allow or prevent water flow through its up-and-down motion; the bonnet is wrapped around this
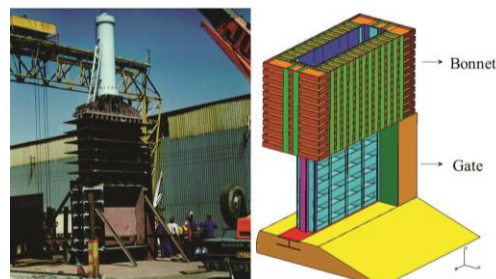

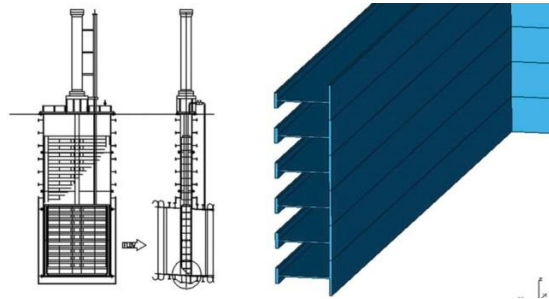Fig. 1 High-pressure slide gate system

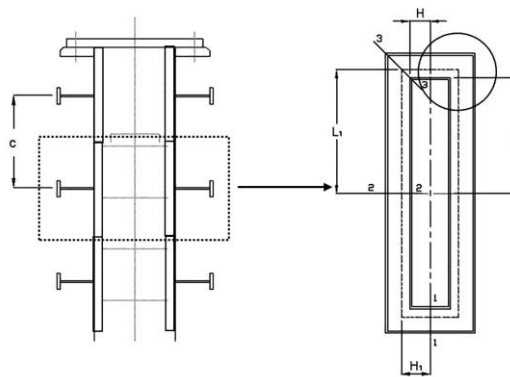Fig. 2 Bonnet structure and the right-angle frames

Fig. 3 Side and top views of bonnet with horizontal girders

gate. The bonnet structure consists of skin plates and horizontal and vertical stiffness guides (Orbanich and Ortega 2013). This structure should be able to support hoisted loads as well as the internal water pressure. The horizontal girder is a structure stacked with a number of wide flanges, as shown in Fig. 2. Fig. 3 shows the side and top views of the bonnet structure, where c is the repeated height of the horizontal girder. The design of the wide flange beam with the proper width of the base flange was based on DIN 19704 (DIN 1976). As shown in Fig. 3(b), L (section 2-3) and H (section 1-3) represent half-lengths of an internal side wall in perpendicular directions loaded directly with water pressure. Similarly, L_1 and H_1 represent the lengths of perpendicular lines passing through the centroid of the cross-section of the horizontal girder.

2.2 Governing equation of corner moment for right-angle frames

In this study, the governing equations were derived by considering the stiffness of the corner part to be infinity. This result was compared with the FEA results to evaluate the errors caused by the assumption. From these empirical errors, the actual corner stiffness can be evaluated by reverse engineering. The corner stiffness for different cross-sectional sizes of the frame can be represented by a single master curve for a specific type of cross-section. The accuracy of the design moments at the centers of the frame can be evaluated by using this corner stiffness and referring to a design equation assuming a finite corner stiffness.

Consider a right-angle frame that is a quarter model of the bonnet structure, as shown in Fig. 4, and the typical formulation for analyzing the conventional bonnet corner part of a slide gate. To
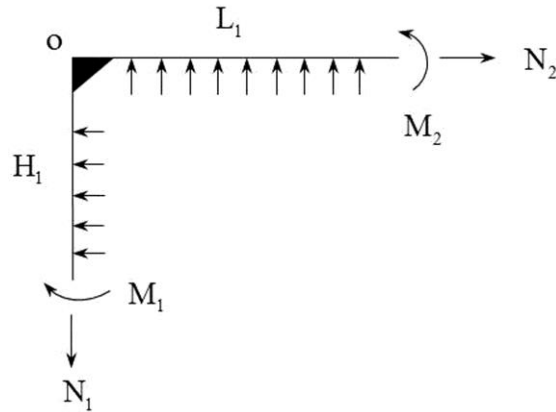
Fig. 4 Free body diagram: quarter part of horizontal girder with rigid corner
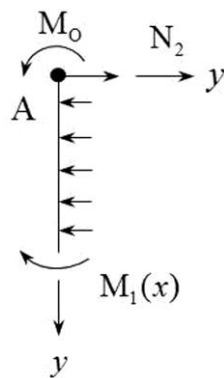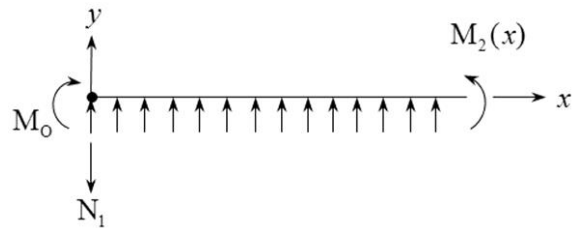

Fig. 5 Free body diagram of section 1-3   Fig. 6 Free body diagram of section 2-3

simplify the problem, the corner stiffness was assumed to be infinite. The internal pressure P was converted to P_H, which is the redistributed load to the neutral plane of the horizontal girder's cross-section area and can be written as

$$P_H = P \times \frac{L+H}{L_1 + H_1} \tag{1}$$

The intensity of load per unit length can be expressed as

$$Q_H = P_H \times c \tag{2}$$

The tensile loads N_1 and N_2 can be expressed as

$$N_1 = Q_H \times L_1 \tag{3}$$

$$N_2 = Q_H \times H_1 \tag{4}$$

The right-angle frame model can be divided into two sections, as shown in Figs. 5 and 6, as

free body diagrams. The bending moment in section 1-3 at point x from o can be obtained by the moment equilibrium, which can be expressed as

$$M_1(x) = M_O + \frac{1}{2}Q_H x^2 - N_2 x \tag{5}$$

The differential equation for the deflection curve is

$$w'' = -\frac{M_1}{EI} \tag{6}$$

where w is the vertical deflection to the section beam. The gradient of deflection can be obtained by integrating Eq. (6), which can be written as

$$w' = \frac{1}{EI}\left(-M_O x - \frac{1}{6}Q_H x^3 + \frac{1}{2}N_2 x\right) + C_1 \tag{7}$$

The boundary conditions of the vertical section of beam are

$$w'(0) = \theta_A \tag{8}$$

$$w'(H_1) = 0 \tag{9}$$

where θ_A is the deflection angle at point A. By applying these boundary conditions to Eq. (7), the following equation should be satisfied

$$0 = -M_O H_1 - \frac{1}{6}Q_H H_1^3 + \frac{1}{2}N_2 H_1^2 + \theta_A EI \tag{10}$$

Similarly, the bending moment in section 2-3 at point x from o can be obtained from

$$M_2(x) = M_O + \frac{1}{2}Q_H x^2 - N_1 x \tag{11}$$

The differential equation for the deflection curve is expressed in Eq. (12), where the sign of the right-hand term changes from negative in Eq. (6) to positive. The reason for this is that a different sign of moment was used for each section to maintain overall consistency of the sign of moments throughout the structure. The deflection angle, which is expressed by Eq. (13), is obtained by substituting Eq. (11) into Eq. (12).

$$w'' = \frac{M_2}{EI} \tag{12}$$

$$w' = \frac{1}{EI}\left(M_O x + \frac{1}{6}Q_H x^3 - \frac{1}{2}N_1 x^2\right) + C_2 \tag{13}$$

where θ_B is the deflection angle at point B. After the boundary conditions are applied

$$w'(0) = \theta_B \tag{14}$$

$$w'(L_1) = 0 \tag{15}$$

Eqs. (13) and (16) must be satisfied.

$$0 = M_O L_1 + \frac{1}{6} Q_H L_1^3 - \frac{1}{2} N_1 L_1^2 + \theta_B EI \tag{16}$$

From the condition of infinite corner rigidity, Eq. (17) needs to be satisfied:

$$\theta_A = \theta_B \tag{17}$$

From this, the corner moment M_O can be obtained based on the assumption of infinite corner stiffness as follows

$$M_O = \frac{Q_H (L_1^3 + H_1^3)}{3(L_1 + H_1)} \tag{18}$$

Design equation set I for the moments at the centers of the frame can be expressed by Eqs. (19) and (20)

$$M_1(H_1) = M_O + \frac{1}{2} Q_H H_1^2 - N_2 H_1$$
$$= \frac{Q_H (L_1^3 + H_1^3)}{3(L_1 + H_1)} - \frac{1}{2} Q_H H_1^2 \tag{19}$$

$$M_2(L_2) = M_O + \frac{1}{2} Q_H L_1^2 - N_2 L_1$$
$$= \frac{Q_H (L_1^3 + H_1^3)}{3(L_1 + H_1)} - \frac{1}{2} Q_H L_1^2 \tag{20}$$

Therefore, the design of right-angle frames has assumed the corner stiffness to be infinite.

This design was extended to the case of finite corner stiffness K_C. The formula for the corner moment M_C can be expressed as (Kwon)

$$M_C = \frac{Q_H (L_1^3 + H_1^3)}{3(L_1 + H_1) + 3EI / K_C} \tag{21}$$

$M_1(H_1)$ and $M_2(L_1)$ in design equation set I need to be changed by replacing M_O with M_C, where M_C converges to M_O if M_C approaches infinity. Design equation set II, which is for the moments at the centers of the frame assuming finite corner stiffness, can be expressed by Eqs. (22) and (23). Once M_C is given as in Eq. (21), it replaces M_O in Eq. (19) and Eq. (20) to give following equations, where, M_C could be obtained if we attach a torsional spring of the stiffness K_C at point O in Fig. 4 instead of the rigid bracket.

$$M_1(H_1) = M_C + \frac{1}{2} Q_H H_1^2 - N_2 H_1$$
$$= \frac{Q_H (L_1^3 + H_1^3)}{3(L_1 + H_1) + 3EI / K_C} - \frac{1}{2} Q_H H_1^2 \tag{22}$$

$$M_2(L_2) = M_C + \frac{1}{2}Q_H L_1^2 - N_2 L_1$$

$$= \frac{Q_H(L_1^3 + H_1^3)}{3(L_1 + H_1) + 3EI/K_C} - \frac{1}{2}Q_H L_1^2 \qquad (23)$$

3. Comparison between K–M equation and FEM result

Fig. 7 shows the FE model, which is composed of many beam elements. The commercial program NISA II (EMRC 1994) was used to solve the linear static problem under internal pressure. Table 1 lists the geometry, material properties, and applied pressure of this model, where a and b denote the width and thickness, respectively, of the rectangular cross-section. A torsion spring was applied to the corner to connect two beams and simulate the corner stiffness of the right-angle frame. Fig. 8 compares the theoretical result from Eq. (21) using the $K_C\_M_C$ relation and the FEA result with the torsional spring. As shown in the graph, the theoretical result was consistent with the FEA result, which validates the former. When the torsion stiffness K_C is

Table 1 Geometry, material properties, and applied pressure

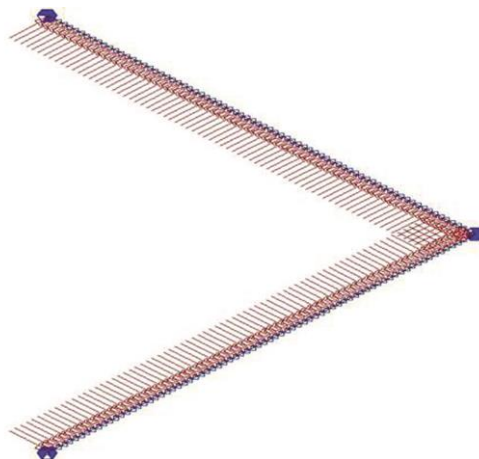|		
Length L_1	L_1 (mm)	1500
Length H_1	H_1 (mm)	1500
Height of the cross-section	a (mm)	150
Width of the cross-section	b (mm)	20
Young's modulus	E (GPa)	207
Poisson's ratio	v	0.3
Inner pressure	P (MPa)	1
Section modulus	I (mm^4)	5,625,000

Fig. 7 Finite element beam model of horizontal girder with corner torsional spring of stiffness M_C using NISA II
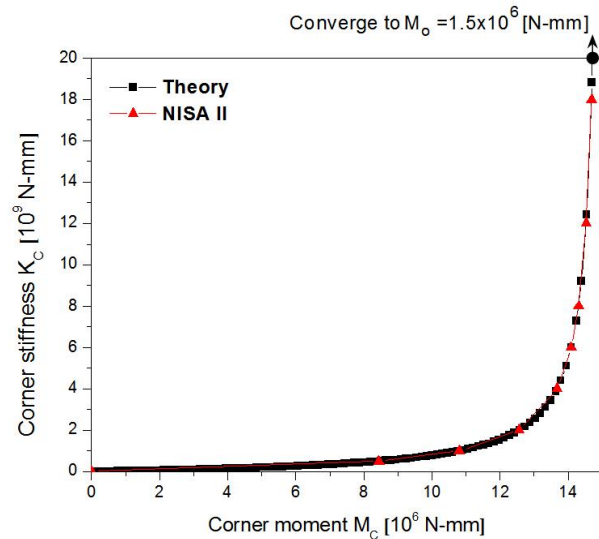
Fig. 8 Relationship between corner stiffness K_C and corner moment M_C

infinitely large (Fig. 8), the corner moment can be observed, and M_C converges to M_O=1.5×10^7 N-mm.

Until now, the corner stiffness has typically been assumed to be infinite and used to calculate the corner moment and following design moments, as shown in design equation set I. However, without an accurate evaluation of the corner stiffness, the correct corner moment and following design moments at the centers of the frame cannot be obtained with design equation set II.

4. Master curves for empirical corner stiffness and application to design equation set II

As discussed in the previous section, design equation set I was derived based on the assumption of a rigid corner. As an extension, design equation set II was derived based on the assumption of finite corner stiffness. For correct evaluation of the design moments, determining the correct corner moment is needed.

The primary problem raised above was considered for two types of cross-sections: rectangular and wide flange beams. The simple approach is as follows. First, the bending stresses are compared using design equation set I and FEA. The error is used to reverse-engineer the required finite corner stiffness that can nullify the errors for different dimensions of the cross-section of a given type. These empirically obtained data points on the corner stiffness can be arranged as a function of the slenderness ratio and represented by a single master curve.

4.1 Master curve for right-angle frame of rectangular cross-section

The bending stresses at point A of Fig. 9 for the 18 conditions given in Table 2 were calculated using design equation set I with the rigid corner stiffness. These stresses were compared with the FEA results. Fig. 10 shows the difference between the theoretical stresses and the FEA results in

terms of the slenderness ratio. A small difference in the stresses resulted in a beam with a large slenderness ratio. On the other hand, a smaller slenderness ratio of the beam produced a large difference (>10%) in the stresses. In other words, Eq. (18) can be used with a slenderness ratio of >50, but the error is significant for a slenderness ratio of <50. Fig. 11 shows the dimensionless value of $\tilde{K}_C^{RECT}$ according to the slenderness ratio. This master curve was obtained by reverse-engineering to nullify the errors in Fig. 10.

Table 2 Rectangular beam samples [mm]

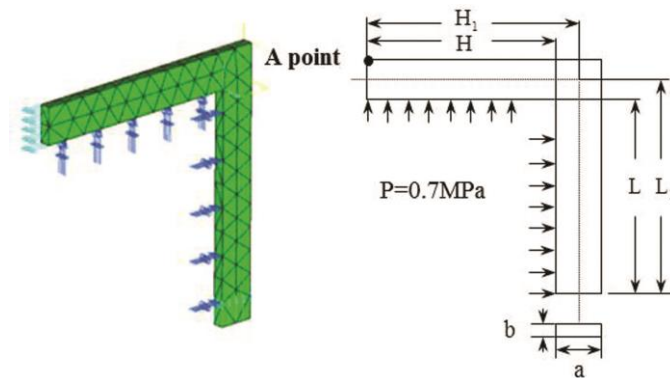| Type	*a*	*b*	Size (*L*=*H*)
S_1	80	25	500, 1000, 1500, 2000,
S_2	90	22	2500, 3000
S_3	100	20	*P*=0.7 MPa, *E*=207 GPa

Fig. 9 Boundary conditions and schematic diagram of horizontal girder with rectangular cross-section
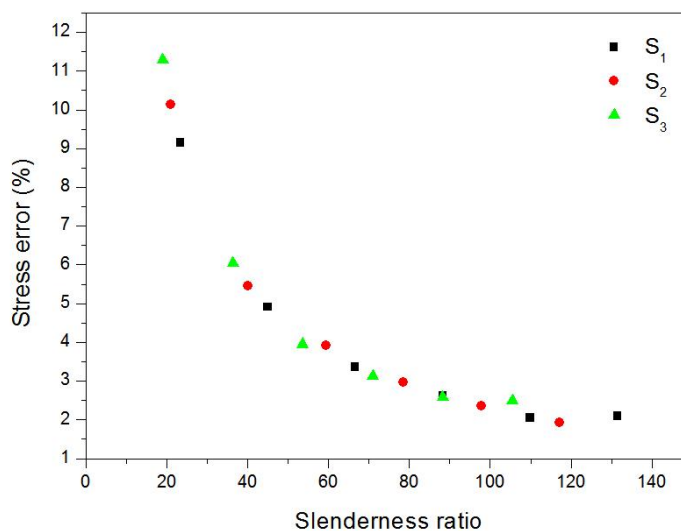

Fig. 10 Error between theoretical stress (point A) assuming rigid corner stiffness and FEA versus slenderness ratio of beams with rectangular cross-section
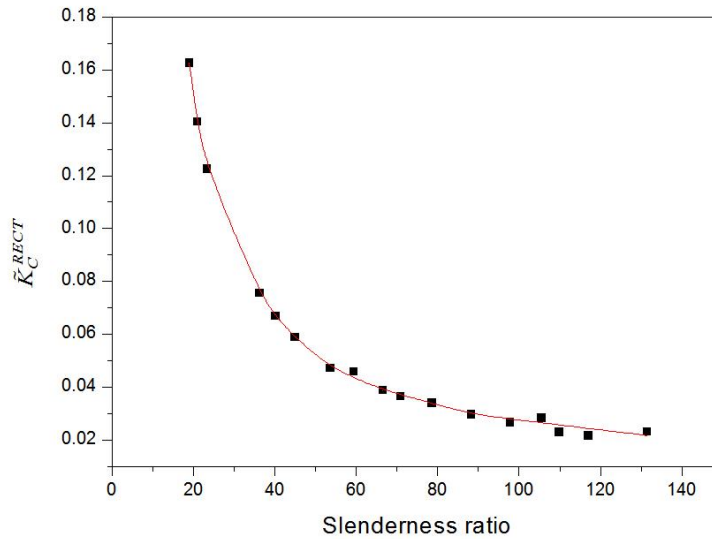
Fig. 11 Master curve for $\tilde{K}_C^{RECT}$ versus slenderness ratio of beams with rectangular cross-section

When the slenderness ratio and geometric data are given, the empirical dimensionless corner stiffness is taken from the master curve of Fig. 11. With this dimensionless stiffness, the corner moment can be evaluated by using Eq. (23).

$$\tilde{K}_C = \frac{K}{K_C} = \frac{EI}{lK_C} \tag{24}$$

K_C=stiffness at the corner
K=stiffness for the beam
E=Young's modulus
I=moment of inertia of the section
l=length of the beam to measure

$$M_C = \frac{Q_H(L_1^3 + H_1^3)}{3[(L_1 + H_1) + l\tilde{K}_C]} \tag{25}$$

The design moments can be calculated by using design equation set II, and Eq. (23) can be used to compute the bending stresses at the centers of the right-angle frame of the rectangular cross-section. The overall procedure is given below.

• Evaluate frame properties.
  - Area: A
  - Moment of inertia: I
  - Radius of gyration: k
  - Slenderness ratio: $\lambda = l/k$
  - Read the stiffness ratio $\tilde{K}_C$ from the master curve for the given slenderness ratio λ.

• Compute the corner moment M_C for the given load using the stiffness ratio $\tilde{K}_C$.

• Compute the center moments M_{1max} and M_{2max} using the corner moment M_C.
• Compute bending stresses at the girder centers by using N, M_{1max}, and M_{2max} to check the safety factors.

For example, in the case that each branch of the frame differs in length, the overall corner stiffness $\tilde{K}_C$ can be obtained in analogy with the contact of springs in series as follows

$$\tilde{K}_C^{Overall} = \frac{1}{1/2\tilde{K}_{C1}+1/2\tilde{K}_{C2}} = \frac{2\tilde{K}_{C1}\cdot\tilde{K}_{C2}}{\tilde{K}_{C1}+\tilde{K}_{C2}} \tag{26}$$

where $\tilde{K}_{C1}$ and $\tilde{K}_{C2}$ are the corner stiffness values of frames having equal branches.

4.2 Master curve for right-angle frame of wide flange beam

Before the master curve can be obtained for the right-angle frame of a wide flange beam, the errors between the results from design equation set I and FEA were first calculated for different web sizes and for different flange sizes, as discussed in the sections below.

4.2.1 Comparison between design equation set I and FEA for different web lengths of wide flange beam

The bending stresses at point A in Fig. 12 for the 18 conditions given in Table 3 were calculated using design equation set I with rigid corner stiffness. These stresses were compared with the FEA results. Fig. 13 shows the difference between the theoretical stresses and the FEA results in terms of the slenderness ratio. The errors in bending stresses were large regardless of the slenderness ratio. In other words, a design based on the assumption of rigid corner stiffness may result in an error of more than 15%.

Table 3 Wide flange beam samples of different web lengths [mm]

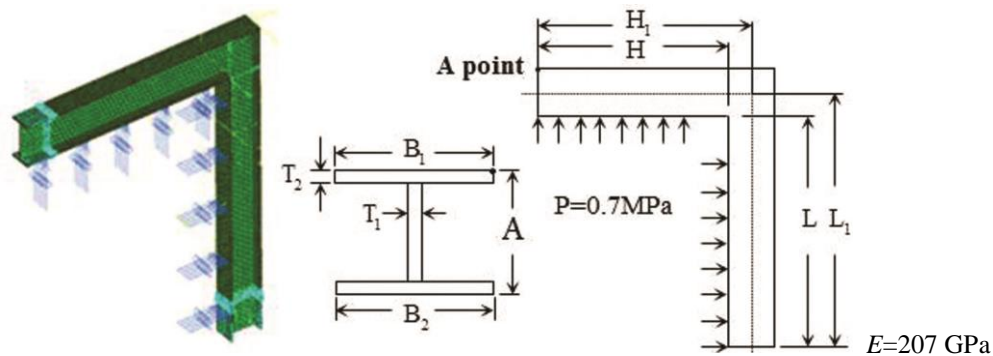| Type	A	$B_1=B_2$	T_1	T_2	Size ($L=H$)
S_1	200	200	8	12	500, 1000, 1500,
S_2	300	200	8	12	2000, 2500, 3000
S_3	400	200	8	12	P=0.7 MPa, E=207 GPa

Fig. 12 Boundary conditions and schematic diagram of the wide flange beam model of variable size of web A
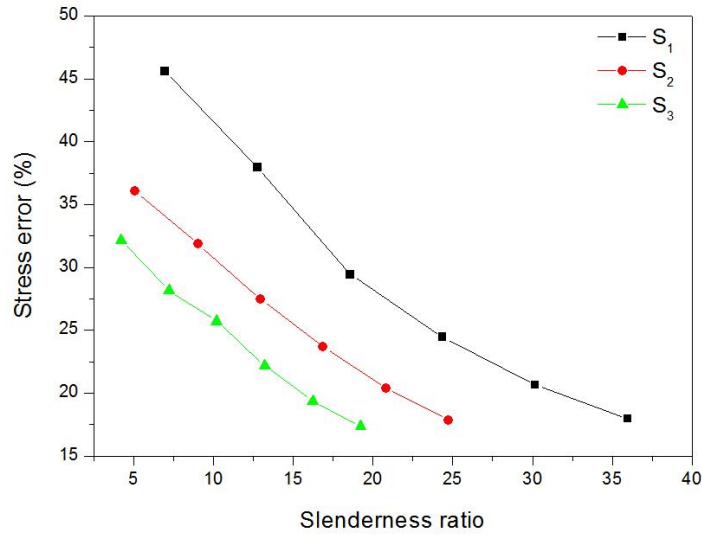
Fig. 13 Error between theoretical center stress (point A) assuming rigid corner stiffness and FEA as function of slenderness ratio of wide flange beams for different lengths of web A

Table 4 Wide flange beam samples with upper flange of variable size [mm]

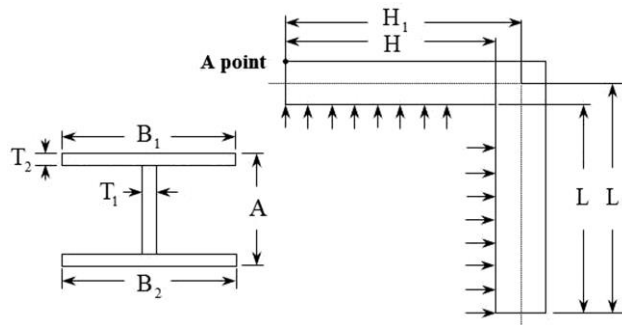| Type	A	B_1	B_2	T_1	T_2	Size (L=H)
S_4	200	200	200	8	12	500, 1000, 1500,
S_5	200	150	200	8	12	2000, 2500, 3000
S_6	200	100	200	8	12	P=0.7 MPa, E=207 GPa

Fig. 14 Schematic diagram of wide flange beam model with upper flange B_1 of variable size

4.2.2 Comparison between design equation set I and FEA for different flange lengths of wide flange beam

The bending stresses at point A in Fig. 12 for the 24 conditions given in Table 4 were calculated using design equation set I with rigid corner stiffness. These stresses were compared with the FEA results. Fig. 15 shows the difference between the theoretical stresses and the FEA results in terms of the slenderness ratio. The errors in the bending stresses were considerable regardless of the slenderness ratio. In other words, a design based on the assumption of rigid corner stiffness may result in an error of more than 10% in most cases. Fig. 16 shows the

dimensionless value of $\tilde{K}_C^{WIDE}$ according to the slenderness ratio. This master curve was obtained by reverse-engineering to nullify the errors in Figs. 13 and 15.

When the slenderness ratio and geometric data are given, the empirical dimensionless corner stiffness is read from the master curve of Fig. 16. With this dimensionless stiffness, the corner moment can be evaluated by using Eq. (23). The design moments can be evaluated by using design equation set II and Eq. (23) to calculate the bending stresses at the centers of the right-angle frame of the wide flange beam. The overall procedure is the same as that given above for the case of a rectangular cross-section.
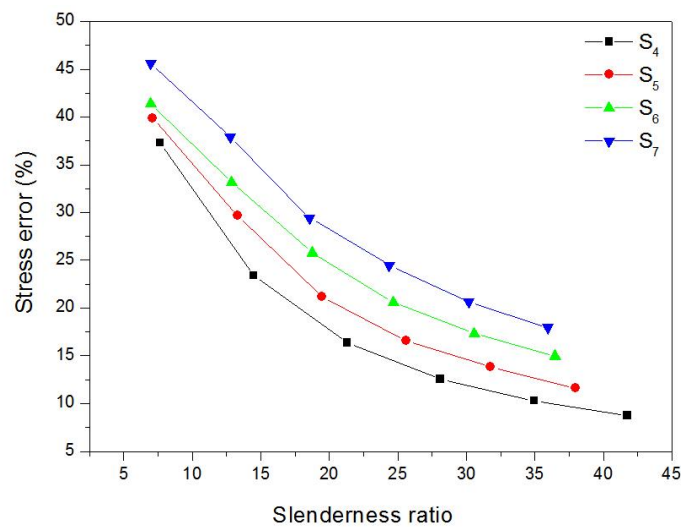

Fig. 15 Error between theoretical center stress (point A) assuming rigid corner stiffness and FEA as function of slenderness ratio of wide flange beam for different lengths of upper flange B_1
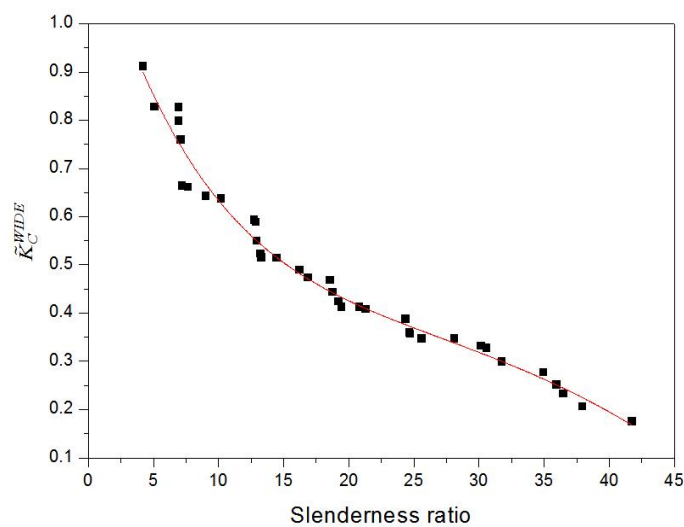

Fig. 16 Master curve for $\tilde{K}_C^{WIDE}$ versus slenderness ratio of wide flange beam
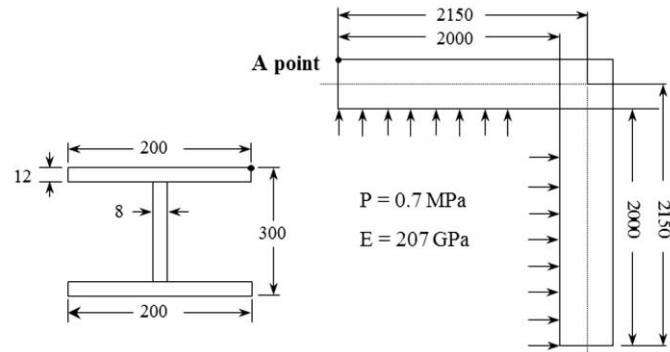
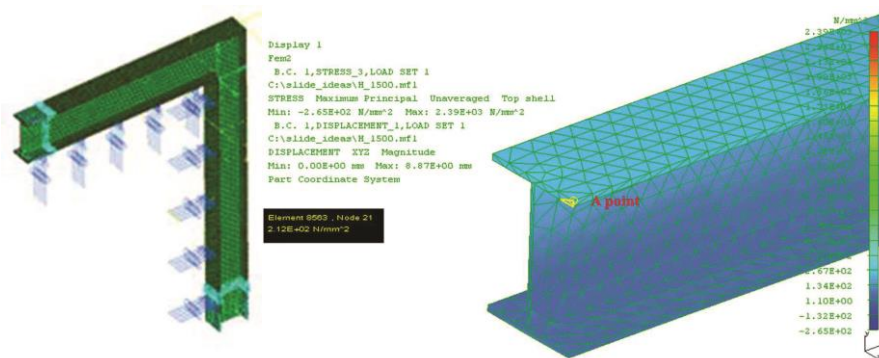Fig. 17 Schematic diagram of example wide flange beam

Fig. 18 Boundary conditions of model and result at point A

4.2.3 Example of using $\widetilde{K}_C^{WIDE}$ table for wide flange beam

A structure comprising a wide flange beam and loaded with an internal pressure of 0.7 MPa was considered to test the validity of the master curve in Fig. 16. Fig. 17 shows the geometric data of the structure and the boundary conditions. Using design equation set I, the corner stress for the wide flange beam was 265 MPa. Using the master curve and design equation set II, the corner stress was 216 MPa. The reference stress according to FEA was 214 MPa, as shown in Fig. 18.

The error of 23% using the former theoretical method was significantly reduced to 0.95% using design equation set II, which assumes finite corner stiffness, and the master curve for the empirical corner stiffness.

5. Conclusions

Until now, the stiffness of the corner of a right-angle frame has been assumed to be infinite. However, this assumption sometimes leads to a considerable error. Two master curves for the dimensionless corner stiffness were obtained by comparing stresses using the derived corner moment for rigid stiffness and FEA. Very accurate design moments and bending stresses of the right-angle frame were determined by applying the empirical corner stiffness to design equation set II.

The results of this study are summarized as follows.

• A master curve for the dimensionless corner stiffness was obtained for the right-angle frame of a rectangular cross-section. This can be used to evaluate the corner moment based on the assumption of finite corner stiffness and to more accurately evaluate the design moments and stresses of right-angle frames.

• A master curve for the right-angle frame of a wide flange beam was obtained. This can be used to evaluate the corner and design moments of wide flange beams having various dimensions to analyze and design right-angle frames more accurately.

• For the right-angle frame of a rectangular cross-section with a slenderness ratio of over 50, design equation set I can be used without considerable error. On the other hand, the assumption of rigid corner stiffness leads to significant error for a rectangular cross-section with a slenderness ratio of less than 50 and most cases of wide flange beams. Therefore, the use of the master curves is strongly recommended.

Acknowledgments

References

DIN 19704 (1976), *Hydraulic Steel Structures Criteria for Design and Calculation*, Germany.

EMRC (1994), *NISA II - User's manual*.

Hydraulic Gate and Penstock Association (1986), *Technical Standards for Gates and Penstock.*

Kwon, Y.D., Jin, S.B. and Kim, J.Y. (2004), "Local zooming genetic algorithm and its application to radial gate support problems", *Struct. Eng. Mech.*, **17**(5), 611-626.

Kwon, Y.D. "Analysis of the right-angle frame with round corner considering a finite corner stiffness". (in preparation)

Kwon, Y.D., Kwon, S.B., Goo, N.S. and Jin, S.B. (2000), "Optimal location of support point for weight minimization in radial gate of dam structure", *Trans. KSME (A)*, **2**(1), 492-497.

Lewin, J. (2001), *Hydraulic Gates and Valves*, Inst. of Civil Engineers Publication, London.

Orbanich, C.J. and Ortega, N.F. (2013), "Analysis of elastic foundation plates with internal and perimetric stiffening beams on elastic foundations by using finite differences method", *Struct. Eng. Mech.*, **45**(2), 169-182.

Reismann, H. and Pawlik, P.S. (1980), *Elasticity-Theory and Applications*, John Wiely & Sons, Inc., New York.

Shariatmadar, H. (2011), "Dam-reservoir-foundation interaction effects on the modal characteristic of concrete gravity dams", *Struct. Eng. Mech.*, **38**(1)**,** 65-79.

Timoshenko, S. and Goodier, J. (1970), *Theory of Elasticity*, 3rd Edition, McGraw Hill, New York.

Ugural, A. and Fenster, S.K. (2003), *Advanced Strength and Applied Elasticity*, 4th Edition, Prentice Hall, London.